PERFORMANCE COMPARISON OF RUDDER PROFILES FOR LATERAL STEERING OF SEISMIC STREAMERS

Jan Vidar Grindheim[1,2,3*]

jg@geograf.no

Inge Revhaug[2]

inge.revhaug@nmbu.no

Joel Sena Sales Junior[3]

joel@oceanica.ufrj.br

Mohammad Mobasheramini[3]

mohammad.amini@oceanica.ufrj.br

Egil Pedersen[4]

egil.pedersen@ntc-as.no

Peder Solheim[1]

peder@geograf.no

Abstract

Seismic streamers are utilized extensively for offshore petroleum exploration. Optimal steering of the streamers is one important aspect of improving the efficiency of seismic operations. A simulation study has been performed for comparing the efficiency of symmetric rudder profiles for lateral steering of towed underwater seismic streamers. The profiles are in two categories: NACA symmetrical profiles and Schilling profiles. In the first set of simulation runs, profiles proprietary to Laboratório de Ondas e Correntes (LOC) at

[1]Geograf AS, Strandgt. 5, NO-4307 Sandnes, Norway.

*Corresponding author. E-mail: jg@geograf.no

[2]Faculty of Science and Technology, Norwegian University of Life Sciences (NMBU), IMT, P.O.B. 5003, NO-1432 Ås, Norway.

[3] Laboratório de Ondas e Correntes (LOC) at UFRJ/COPPE, Federal University of Rio de Janeiro, Rio de Janeiro 22241-160, Brazil.

[4] Department of Engineering Science and Safety, UiT - The Arctic University of Norway, Hansine Hansens veg 18, NO-9037 Tromsø, Norway.

UFRJ/COPPE are utilized. Lift- and drag curves based on both laboratory experiments performed at LOC and Computational Fluid Dynamics (CFD) are utilized. In the second set of simulation runs, a series of profiles from Nguyen & Ikeda (2014) are utilized.

The performance data for the various profiles have been implemented in a seismic streamer steering simulator. The same simulation run is run for each of the rudder profiles, where the simulator is set to follow a predefined path. The aim is for the streamer to follow the predefined path as closely as possible with the least amount of rudder drag. Based on the simulation data it is suggested that the Schilling rudders have higher steering performance compared to the NACA profiles.

Keywords: *Seismic Streamer Steering, Hydrodynamics, Schilling Rudder, CFD, Cable Dynamics*

INTRODUCTION

Seismic towed underwater streamers are used extensively for offshore petroleum exploration. A number of streamers with numerous seismic sensors installed are towed behind a vessel (Fig. 1). At the tail, a tailbuoy is attached for identification to other traffic and for facilitating installation of positioning and other devices, as well as assuring streamer tension. At fixed time intervals in the order of 10 seconds, an array of pneumatic devices fires, generating sound waves. The sound waves penetrate the water column and underlying seabed strata. Subsequently, reflected pressure waves are recorded by sensors at the towed streamers. The collected data can then be processed to generate images of the hydrocarbon structures in the area.

The streamers also contain instruments such as positioning devices and tension meters, and they have ballast weights installed to reduce depth control workload. While depth control of streamers has been conducted for decades, more recently lateral steering has also become standard for the industry. Steering birds for combined depth and lateral steering, with variations of between 2 and 4 rudders, are mounted at intervals along the streamer.

Improved lateral steering can increase survey efficiency by reducing the risk of tangling resulting from narrower streamer separation and longer streamers, and by improving 4D seismic repeatability, where the streamers follow the path of historic surveys (Grindheim et al., 2017a). In general rudder drag should be minimized as the steering induced noise reduces the seismic signal to noise ratio. Additionally, turn maneuvers in seismic surveys are time consuming and expensive, and increased lateral control will reduce turn time and expense.

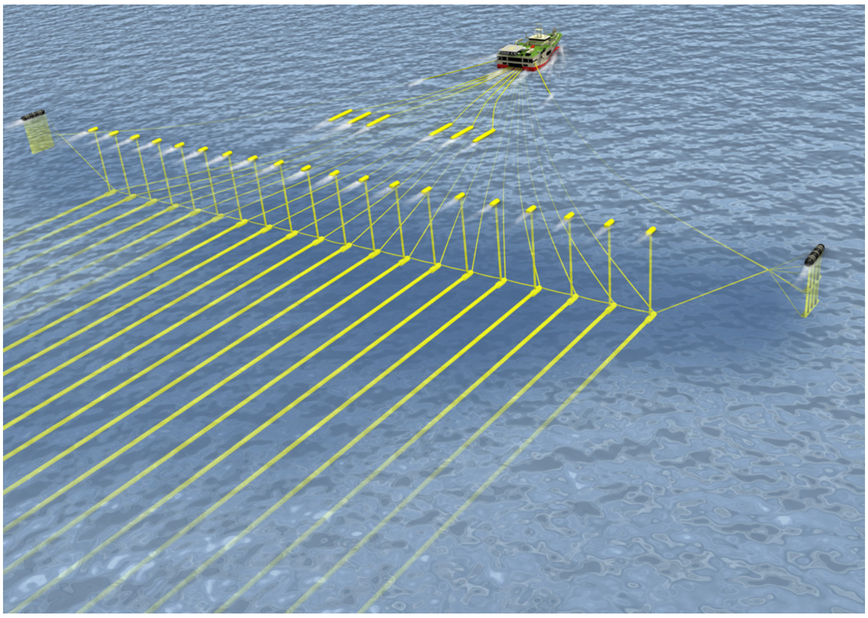

Fig. 1: 3D marine seismic survey configuration. (A courtesy of Petroleum Geo-Services.)

The objective of the present work is to model rudder designs that reduce rudder drag and increase lift. The improved rudder design is to be compatible with existing production bird cores. Some contemporary birds utilize detachable wings, facilitating wing design changes.

The Schilling rudder has been shown to potentially increase maneuverability of ships substantially compared to conventional rudder designs (Bingham & Mackey, 1987). This improved rudder design was developed by Karl Schilling and first fitted on a seagoing vessel in 1975. The concept being similar to the Gurney flap, it employs a fishtail shape at the trailing edge. The increase in lift is attributed to the high pressure developing at the concave face on the rudder pressure side (Nguyen & Ikeda, 2014).

Nagarajan & Hasegawa (2008) performed a simulation study on rudder performance for a very large crude carrier, concluding that the Schilling rudder could potentially increase the maneuverability and reduce fuel consumption compared to a conventional mariner rudder.

For seismic streamer steering, more conventional rudder designs are generally employed. This study aims at investigating potential performance benefits associated with utilizing Schilling rudder designs compared to conventional rudder design like the NACA series symmetric profiles. Some modern streamer steering birds employ detachable wings, hence an improved rudder design could be implemented on existing bird designs (Grindheim et al., 2017b).

Schilling rudders tend to give increased maximum lift coefficients, which could be beneficial for seismic steering, especially at line-changes, where the complete spread is turned 180°. Line-changes are time-consuming and costly, thus optimal steering is of great importance for reducing the time to turn (Ersdal, 2004). It is suggested that the Schilling rudder could aid in reducing the time necessary for line-changes by giving increased maneuverability of the streamers.

1 PRESENT STUDY

A simulation study has been performed for comparing the performance for a variety of rudder profiles for lateral steering of a seismic streamer (cable). The rudder profiles are divided into two main categories: Schilling type ("Fishtail") and conventional NACA type. In the simulation, all rudders have equal surface area of S = 0.208 m^2, where S is the upper surface area. Since the profiles are symmetric, also the lower surface area will be equal to S.

Lift- and drag coefficient (C_L and C_D, respectively) curves for the rudder profiles utilized in the present simulation study are presented in Fig. 10. C_L and C_D are defined as:

$$C_L = \frac{L}{q_\infty S} \qquad C_D = \frac{D}{q_\infty S} \tag{1}$$

where q_∞ is the dynamic pressure defined as:

$$q_\infty = \tfrac{1}{2}\rho_\infty V_\infty{}^2 \tag{2}$$

∞ signifies free stream value, L is lift, D is drag, V is fluid velocity, ρ is fluid density and S is wing surface.

The code *FDM_streamer* is utilized for simulations. It solves the six partial differential equations describing the cable dynamics of a towed underwater cable (Eq. (3)) using the Finite Difference Method. The streamer's dynamics could be defined by six coupled nonlinear partial differential equations (Burgess, 1991; Grindheim et al., 2017a; Grindheim et al., 2017b):

$$\mathbf{M}\frac{\partial \mathbf{y}}{\partial s} = \mathbf{N}\frac{\partial \mathbf{y}}{\partial t} + \mathbf{q} \tag{3}$$

where

$$\mathbf{y} = \begin{bmatrix} T & v_t & v_n & v_b & \theta & \varphi \end{bmatrix}^{\mathrm{T}} \tag{4}$$

M and **N** are 6x6 matrices, while **q** is a 6x1 vector accounting for hydrodynamic and buoyancy forces, including sea current, which may be unique at each streamer node. There are three equations resulting from the cable kinematics and three equations for the equilibrium of forces.

The hydrodynamic forces are represented by the Morison equation. The model uses a local coordinate system following the cable tangent t, with n and b as the normal (nadir) and bi-normal (horizontal) vectors, respectively. In Eq. (4), v is velocity (m/s), T is cable tension (N), and θ and φ are orientation angles in the horizontal and vertical planes, respectively.

As indicated by its name, *FDM_streamer* is customized for seismic streamers, employing tailbuoy, control birds (rudders), and optionally components installed at the streamer. Parameters such as cable properties, location and properties of birds and components, node spacing in the FDM, environmental properties and sea current can be defined by user.

The cable has 25 rudders uniformly distributed along the cable length, 300 m between each. The cable length is 8000 m, diameter 6 cm, and normal drag coefficient is 1. Cable elasticity is $9.5 \cdot 10^9$ N/m^2, and ρ=1025 kg/m^3 for the surrounding fluid. The streamer has neutral weight in water, while each bird has a weight in water of 10 N. Depth control is not employed in the simulations, hence the cable has a curvature shape in the depth dimension with zero depth at front and tailbuoy (Fig. 2, lower plot). Nominal streamer front tension without birds installed is 20425 N at 2.315 m/s. In the FDM the cable nodes are generally spaced 20 m apart.

The towpoint runs in a straight line at 2.315 m/s, and initially the cable is straight. The cable's reference path is a sine-path with wave height 40 m (i.e. maximum 40 m offset from the straight line) and wave length ca. 3770 m. Time step size is 8 seconds.

Sea current is simulated in the lateral plane. The x- and y-components are uncorrelated, each simulated according to a random walk process in time with white noise of standard deviation 0.02 m/s per timestep (Brown & Hwang, 1997, p. 220). Correlation in distance along cable is implemented by using a two state RTS smoother according to a Gauss-Markov process with standard deviation σ=0.5 m/s^2 and decorrelation distance τ=50 m (Brown & Hwang, 1997, p. 313). The exact same current is utilized for all simulation runs. In the depth dimension, sea current is set to zero. A sample simulation plot is given in Fig. 2.

A PI-controller is utilized for adjusting the rudder deflection for keeping each rudder as close to the predefined sine-path as possible. The PI-controller is tuned individually for each profile at the midpoint of the cable, using the Ziegler-Nichols method.

For each simulation, all rudders installed have the same profile. Initially, the cable is a straight line. Subsequently, the rudders force the cable into the sine path. The towpoint is run for 60 minutes, but only the last 20 minutes are retained, as some initial time is spent "forcing" the cable into the sine path. One 60-minute simulation takes ca. 27 seconds on a standard laptop.

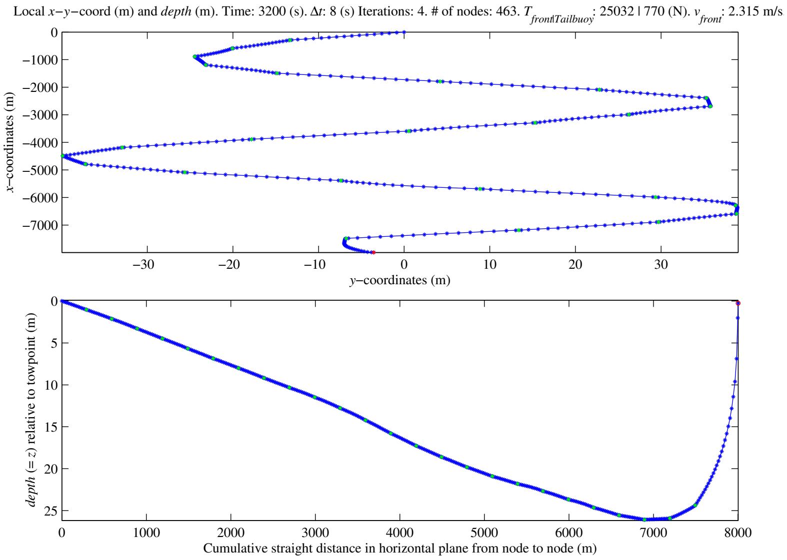

Fig. 2: Coordinate plot for the simulation wit rudder profile Fishtail 04, at simulation time 53.3 minutes. At the upper plot, the cable sine shape can be seen, with "wave height" of ca. 40 m, and some irregularity due to the simulated sea currents. The rudders are shown as green dots.

SIMULATION #1: UTILIZING LOC-PROFILES

The profiles utilized in simulation #1 are proprietary models at Laboratório de Ondas e Correntes (LOC) at UFRJ/COPPE. There are four profiles: NACA0015, NACA-Schilling, Blunt Schilling and Slender Schilling (Fig. 3, Fig. 4).

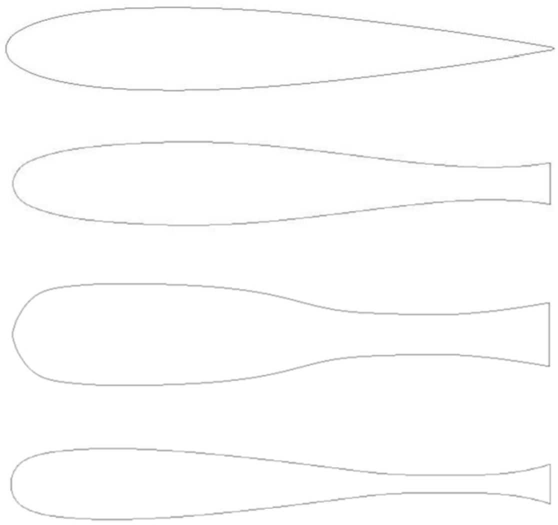

Fig. 3: Profiles utilized in Simulation #2, from Machado et al. (2013). From above, profile #1 is NACA0015, #2 is NACA-Schilling, #3 is Blunt Schilling and #4 is Slender Schilling.

Fig. 4: LOC Schilling profiles (Lima & Fernandes, 2010; Machado et al., 2013). From left: NACA-Schilling, Slender Schilling and Blunt Schilling.

The LOC model dimensions are described in Table 1. For the models, chord length $c \approx 0.20$ m and aspect ratio is 1.75.

Table 1: LOC profiles used in Simulation #1 (Machado et al., 2013) (Fig. 3). Note: *c* is chord length.

Profile	Maximum Thickness	Trailing Edge Thickness
NACA0015	0.15*c*	0.00*c*
NACA-Schilling	0.15*c*	0.09*c*
Slender Schilling	0.13*c*	0.07*c*
Blunt Schilling	0.18*c*	0.11*c*

In Lima & Fernandes (2010), the lift- and drag curves for the four profiles were determined by experiments performed in the current channel at LOC (Machado et al., 2013). The forces were measured using two load cells, one for axial direction and one for normal direction. Channel flow velocity was measured using Acoustic Doppler Velocimetry (ADV). Each test run endured about 3 minutes, and the results were averaged. Water velocity was varied between 0.3 and 0.6 m/s, giving an upper Reynolds number of $1.09 \cdot 10^5$. In Machado et al. (2013), the experimental results were cross-validated with CFD results. NACA experimental results for the NACA0015 profile were utilized in CFD validation (Jacobs & Sherman, 1937).

In the present study, the C_L- and C_D curves for Reynolds number $1.09 \cdot 10^5$ has been utilized for all four profiles, which is the highest Reynolds number for which experimental results are available for the LOC Schilling profiles (Machado et al., 2013). This is less than the seismic operational Reynolds number, but since the present study is a pure comparison of different profiles this should be acceptable. For the NACA0015 profile, the experimental results from Jacobs & Sherman (1937) have been utilized by interpolation between the two closest Reynolds numbers.

For the Schilling profiles, the CFD results from Machado et al. (2013) have been utilized. These CFD results were obtained using grids of 80,000 quadrilateral cells, giving grid independent solution (Machado et al., 2013). The turbulence model utilized was the two-equation SST $\kappa - \omega$ model, as it has been shown to be appropriate for the present problem (Eleni et al., 2012). Convergence limit was set to RMS < 10^{-5}, and steady state results were obtained, assuming incompressible flow. Note that for the NACA0015 profile, the CFD tended to overestimate lift coefficient compared to Jacobs & Sherman (1937) (Machado et al., 2013). Hence CFD lift coefficients for the Schilling profiles may be somewhat overestimated as well.

The resulting C_L- and C_D curves for the four LOC profiles at Re=$1.09 \cdot 10^5$ are shown in Fig. 5. Recall that the LOC-NACA0015 curves are based on the experimental results from Jacobs & Sherman (1937), while the curves for the Schilling profiles are based on the CFD results of Machado et al. (2013).

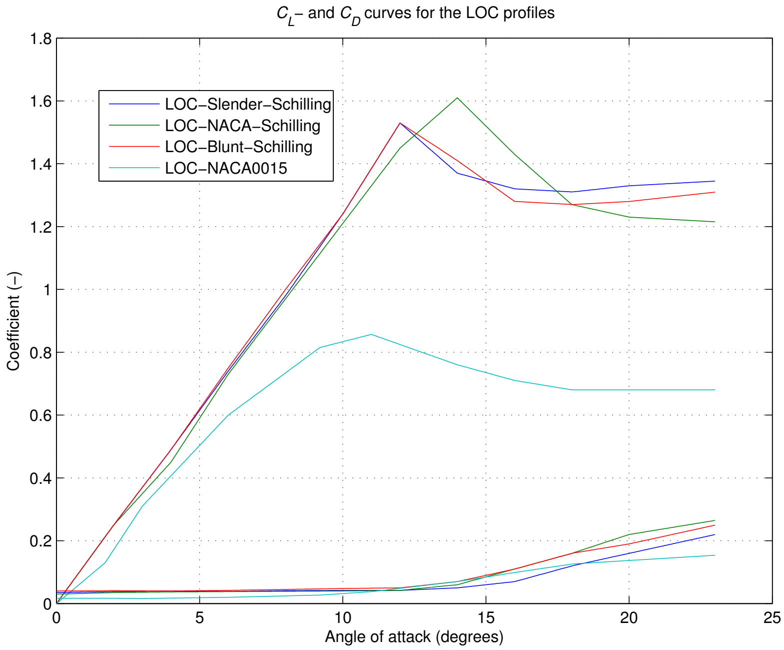

Fig. 5: C_L- and C_D curves for the LOC profiles for Re=1.09·10^5 (C_D are the lower curves). The LOC-NACA0015 curves are based on Jacobs & Sherman (1937), while the curves for the Schilling profiles are based on Machado et al. (2013).

The aim is to minimize both offset from predefined path and drag. The performance factor P_F is defined according to

$$P_F = w_1 \frac{mean(O_m)}{\max(O_m)} w_2 \frac{mean(D_m)}{\max(D_m)} \tag{5}$$

, where O_m is average bird offset from predefined path for each timestep, and D_m is average added drag per timestep, where the initial straight-run streamer drag with no birds installed (20425 N) is subtracted. w_1 and w_2 are weights. In the present study, $w_1 = w_2 = 1$, meaning that equal weight is given to the two performance criteria.

Simulation results are presented in Figs. 6~8.

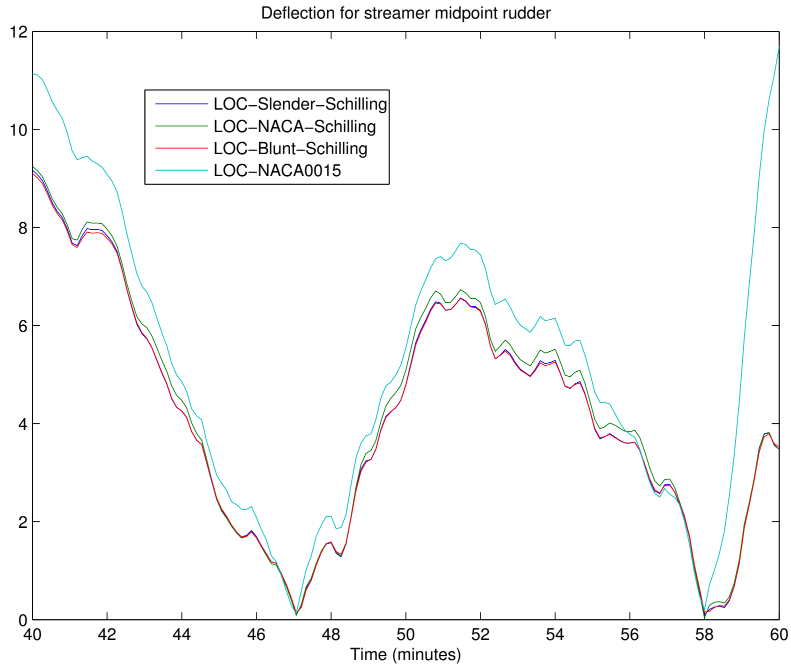

Fig. 6: Simulation #1 (LOC profiles simulation): Rudder deflection for streamer midpoint rudder.

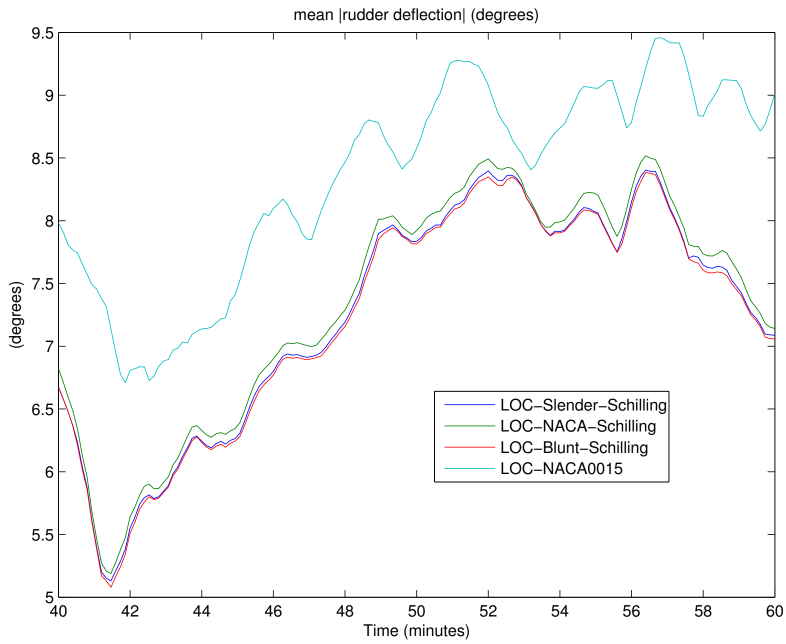

Fig. 7: Simulation #1 (LOC profiles simulation): Mean rudder deflection.

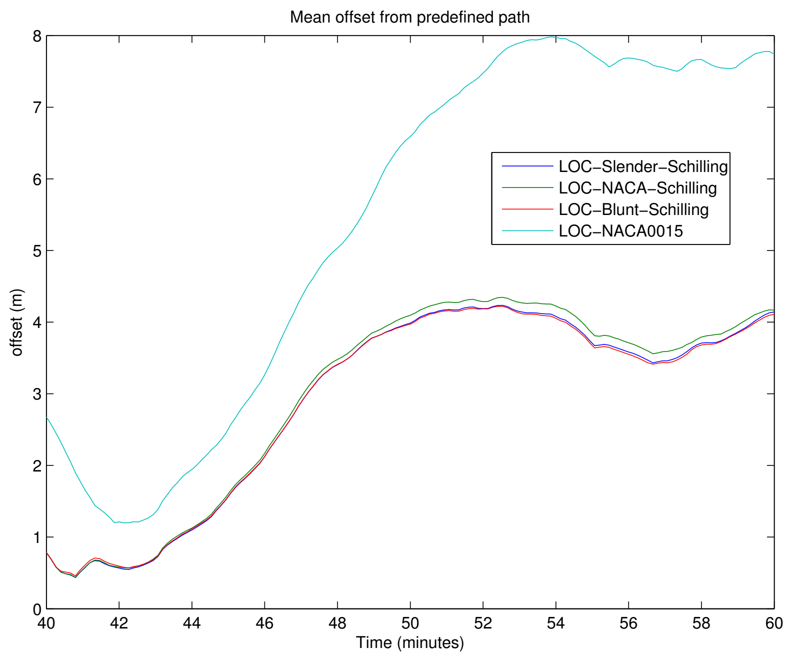

Fig. 8: Simulation #1 (LOC profiles simulation): Mean offset from predefined path for each profile.

In Table 2, the average results from Simulation #1 are presented, sorted according to increasing performance factor P_F (Eq. (5)). Recall that in the mean added drag column (column # 4), the initial straight-run streamer drag with no birds installed (20425 N) is subtracted. The results given in Table 2 are also visualized in Fig. 9.

Table 2: Simulation #1 (LOC profiles simulation): Average results for 20 minutes simulation, sorted according to performance factor P_F (column #2). The reference path has a sine shape with maximum deflection of 40 m from the straight line, and there is a simulated sea current. The aim is to minimize P_F.

Profile	Performance factor P_F	Mean of O_m (i.e. mean offset) (m)	Mean of D_m (i.e. mean added drag) (N)	Mean rudder deflection (deg)	Mean Lift Force (N)
LOC-Slender-Schilling	0.52	2.90	3605	7.2	345
LOC-NACA-Schilling	0.53	2.98	3533	7.3	343
LOC-Blunt-Schilling	0.54	2.89	3702	7.2	346
LOC-NACA0015	0.82	5.38	3036	8.3	299

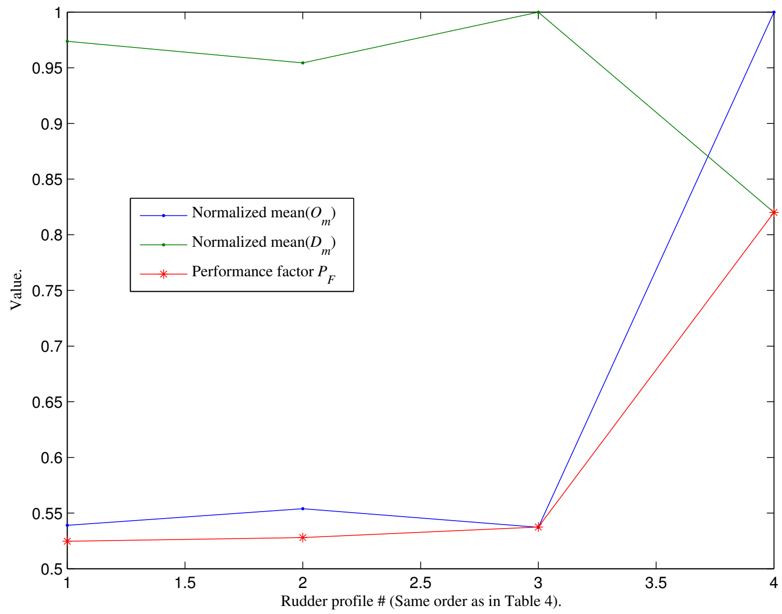

Fig. 9: Simulation #1 (LOC profiles simulation): Plot of normalized offset, normalized total rudder drag and the product of the two (performance factor P_F), for the LOC profiles simulations. The values are also given in Table 2. The *x*-axis corresponds to the row number in Table 2.

For the LOC profiles simulation, the Schilling profiles give the better performance results (Table 2). The Schilling profiles give better steering authority and hence follow the predefined path more closely compared to the NACA profile (Fig. 8). The NACA profile gives lower bird drag, but according to the performance factor P_F (Table 2) the improvement in offset outweighs the increase in drag, assuming equal weight w_1 and w_2 to the two performance criteria (Eq. (5)). For Simulation #1 there is no large difference in performance between the Schilling profiles, but the slender Schilling gives the best result. Recall that the CFD generated lift coefficients for the LOC Schilling profiles may be overestimated, which may impact the performance factor in their favor compared to the NACA0015 profile.

SIMULATION #2: USING RUDDER PROFILES FROM NGUYEN & IKEDA (2014).

Simulation #2 is identical to Simulation #1, except that the rudder profiles are different. In this case, the lift- and drag curves utilized are based on Nguyen & Ikeda (2014), and all are for the identical Reynolds number of $6.0 \cdot 10^6$, since from this point on the curves are no longer significantly affected by Reynolds number. However, this is higher than for seismic streamers, where the Reynolds number is typically around $6.6 \cdot 10^5$, based on a wing chord of 0.3 m and velocity 2.315 m/s. But for a comparison study of different rudder profiles this may be acceptable since all curves are for the same Reynolds number. “Fishtail” is equivalent to Schilling rudder. The profiles utilized are described in Table 3.

Table 3: Profiles used in Simulation #2 from Nguyen & Ikeda (2014). c is chord length.

Name	Maximum Thickness. (*c* is chord length)	Trailing Edge Thickness
Fishtail 01	0.24*c*	0.026*c*
Fishtail 02	0.24*c*	0.05*c*
Fishtail 03	0.24*c*	0.07*c*
Fishtail 04	0.24*c*	0.09*c*
NACA0024	0.24*c*	0.00*c*
Fishtail 05	0.18*c*	0.026*c*
Fishtail 09	0.12*c*	0.026*c*
NACA0012	0.12*c*	0.00*c*

C_L- and C_D curves for the various profiles utilized in Simulation #2 are given in Fig. 10.

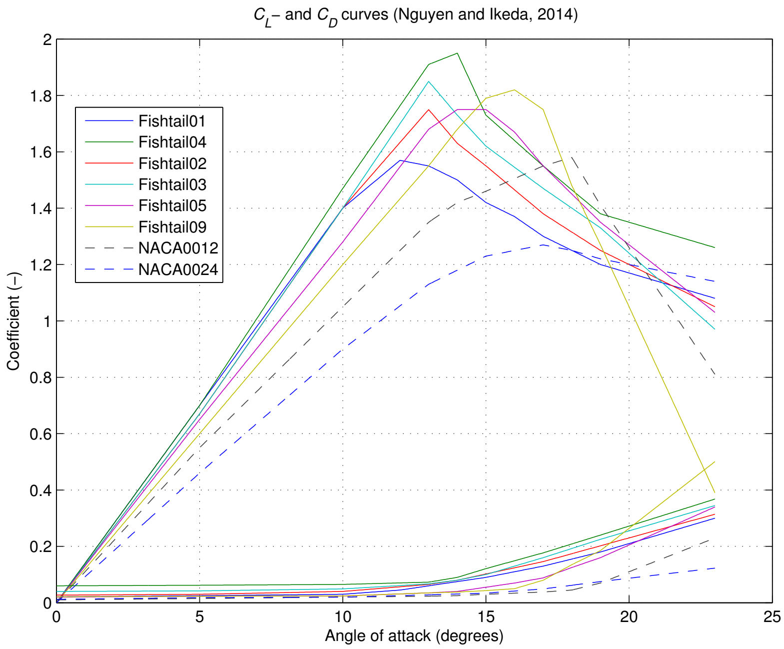

Fig. 10: C_L- and C_D curves for the rudder profiles used in simulation #2, based on Nguyen & Ikeda (2014). C_L are the upper curves, C_D are the lower curves.

The results for Simulation #2 are given in Table 4, sorted according to performance factor P_F.

Table 4: Simulation #2: Average results for 20 minutes simulation, sorted according to P_F (column #2). The reference path has a sine shape with maximum deflection of 40 m from the straight line, and there is a simulated sea current. The aim is to minimize P_F.

Profile	Performance factor P_F	mean(O_m) (i.e. mean offset) (m)	mean(D_m) (i.e. mean added drag) (N)	Mean rudder deflection (deg)	Mean Lift Force (N)
Fishtail01	0.40	2.40	3258	6.8	352
Fishtail02	0.44	2.47	3443	6.9	352
Fishtail05	0.44	2.72	3162	7.1	346
Fishtail09	0.47	2.93	3149	7.3	341
Fishtail03	0.48	2.48	3762	6.9	354
Fishtail04	0.51	2.35	4265	6.8	360
NACA0012	0.52	3.57	2852	7.7	329
NACA0024	0.67	4.57	2865	8.3	312

The results given in Table 4 are visualized in Fig. 11.

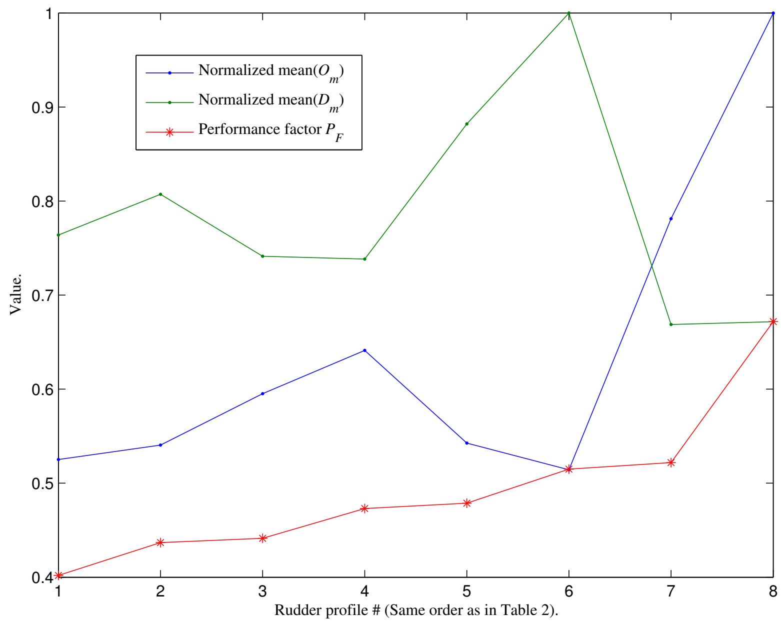

Fig. 11: Simulation #2: Plot of normalized offset, normalized total rudder drag and the product of the two (performance factor P_F). The x-axis corresponds to the row number in Table 4.

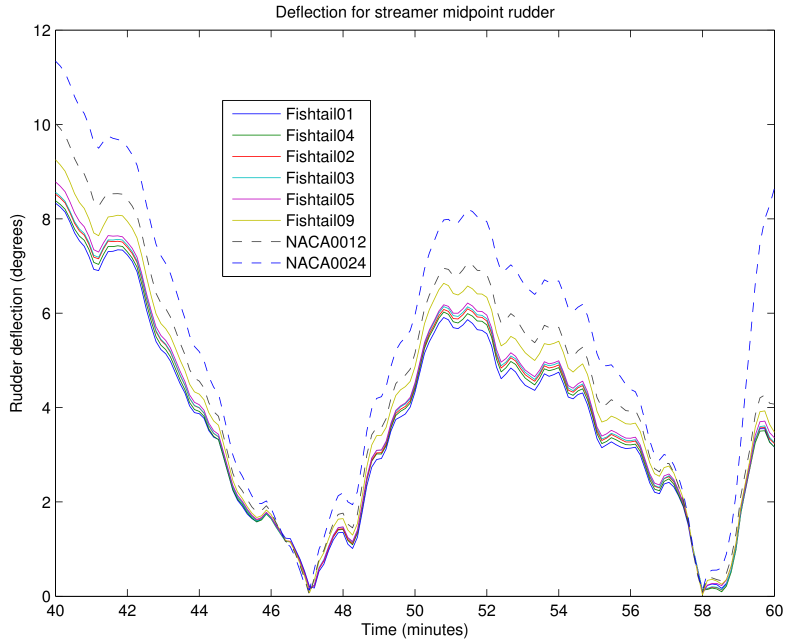

Fig. 12: Simulation #2: Rudder deflection for streamer midpoint rudder.

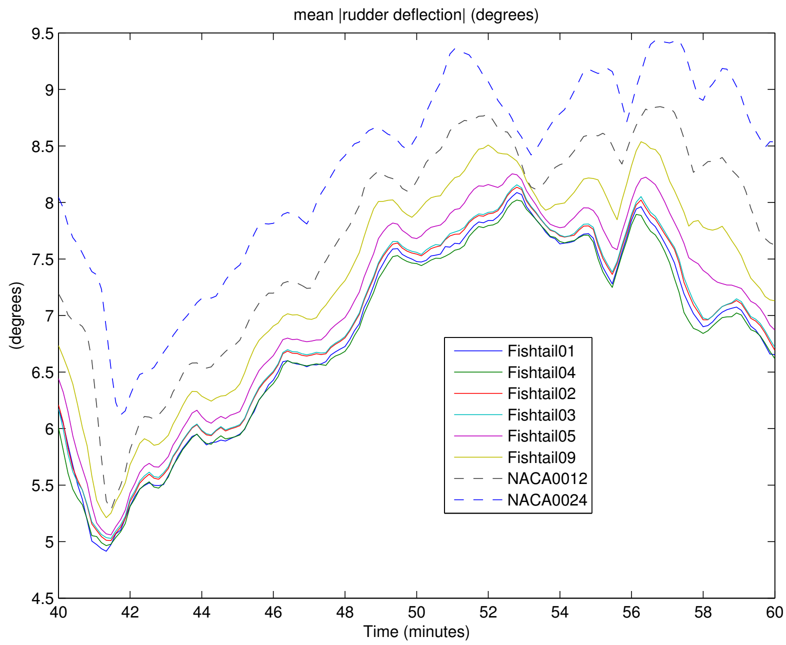

Fig. 13: Simulation #2: Rudder deflection, average of all rudders.

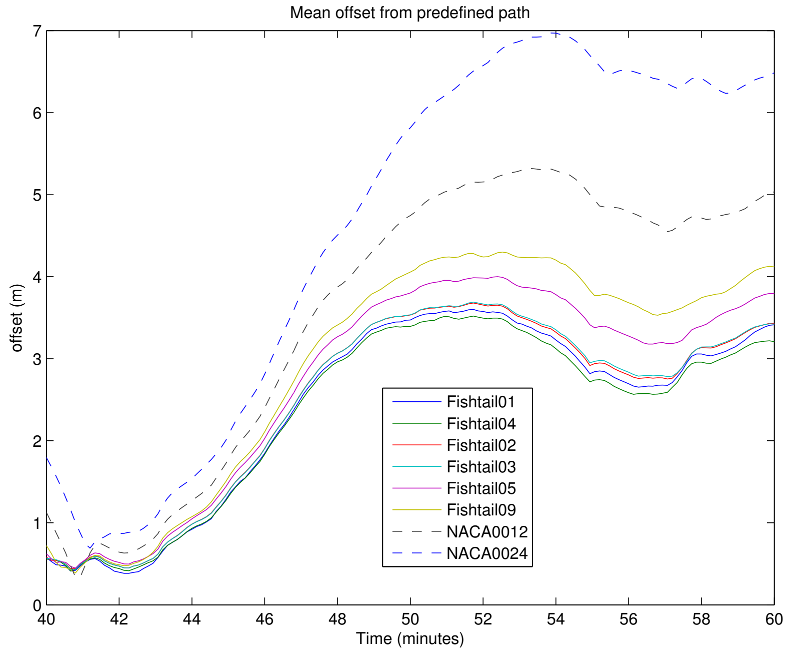

Fig. 14: Simulation #2: Mean offset from predefined path for each of the profiles.

CONCLUSIONS

The Schilling rudder profiles utilized in this study show increased steering authority as they are able to keep the cable closer to the predefined path compared to the conventional rudders. Now, this comes at a slightly higher cost in drag. However, based on the products of normalized path-offset multiplied by normalized drag, the higher steering performance of the Schilling rudders outweighs the cost in higher drag, assuming equal weights to the two criteria (Table 4, Table 2). In general, Schilling type rudders tend to have lower lift-to-drag ratio compared to NACA profiles (Machado et al., 2013).

For Simulation #1 where the LOC profiles are utilized, the Schilling profiles show higher performance compared to the NACA profile. In this case there is no large difference in performance between the three Schilling profiles (Table 2).

For Simulation #2, Fishtail01 gives the best performance factor P_F (Table 2). This is a Schilling profile with small trailing edge, which gives low increase in drag. Increased trailing edge size increases the lift, but at the same time the drag increases significantly (Nguyen & Ikeda, 2014). This is seen from the C_D-curves of Fishtail01~04 (Fig. 10).

It is concluded that Schilling type rudders are able to increase the steering performance of seismic streamers compared to traditional rudder types, when giving equal weight to the two criteria of minimized drag and minimized offset from predefined path.

Acknowledgments

This work is part of an ongoing Industrial PhD at NMBU (Ås, Norway) for Geograf AS (Sandnes, Norway), by the corresponding author. It is funded by Geograf AS and the Research Council of Norway through their Industrial PhD program, project number 234875. Corresponding author is presently on leave to Laboratório de Ondas e Correntes (LOC) at UFRJ/COPPE (Rio de Janeiro, Brazil).

REFERENCES

Bingham, V. P., & Mackey, T. P., 1987. High-Performance Rudders - with Particular Reference to the Schilling Rudder. *Marine Technology,* vol. 24, n. 4, pp. 312-320.

Brown, R. G., & Hwang, P. Y. C., 1997. *Introduction to Random Signals and Applied Kalman Filtering* (3rd ed.). New York, NY: John Wiley & Sons.

Burgess, J. J., 1991. Modeling of Undersea Cable Installation with a Finite Difference Method. *The First International Offshore and Polar Engineering Conference*, pp. 222-227.

Eleni, D. C., Athanasios, T. I. & Dionissios, M. P., 2012. Evaluation of the Turbulence Models for Simulation of the Flow over a National Advisory Committee (NACA) 0012 Airfoil. *Journal of Mechanical Engineering Research,* vol. 4, n. 3, pp. 100-111.

Ersdal, S., 2004. *An Experimental Study of Hydrodynamic Forces on Cylinders and Cables in Near Axial Flow.* PhD thesis, Norwegian University of Science and Technology.

Grindheim, J. V., Revhaug, I., & Pedersen, E., 2017a. Utilizing the EnKF (Ensemble Kalman Filter) and EnKS (Ensemble Kalman Smoother) for Combined State and Parameter Estimation of a 3D Towed Underwater Cable Model. *Journal of Offshore Mechanics and Arctic Engineering*, vol. 139, n. 6, p. 061303.

Grindheim, J. V., Revhaug, I., Pedersen, E., & Solheim, P., 2017b. Modeling, prediction and control of towed marine seismic streamers. *Kart og Plan,* vol. 77, pp. 273-288.

Jacobs, E. N., & Sherman, A., 1937. Report 586 - Airfoil Section Characteristics as Affected by Variations of the Reynolds Number: National Advisory Committee for Aeronautics.

Lima, B. A., & Fernandes, A. C. (2010). *Final Design Project, Naval Architeture (in Portuguese).* Federal University of Rio de Janeiro, Rio de Janeiro.

Machado, L. V., Fernandes, A. C., & Bodstein, G. C. R., 2013. Model Testing and CFD Analysis of 2D Profiles Towards Offshore Applications. *The ASME 2013 32nd International Conference on Ocean, Offshore and Arctic Engineering (OMAE 2013).*

Nagarajan, V., & Hasegawa, K., 2008. Comparison of the mariner Schilling rudder and the mariner rudder for VLCCs in strong winds. *Journal of Marine Science and Technology,* vol. 13, pp. 24-39.

Nguyen, T. V., & Ikeda, Y., 2014. Development of Fishtail Rudder Sections with Higher Maximum Lift Coefficients. *The Twenty-fourth (2014) International Ocean and Polar Engineering Conference*.